

A new torsion pendulum for testing the limits of free-fall for LISA test masses

A Cavalleri¹, G Ciani^{2,3}, R Dolesi^{2,3}, A Heptonstall^{4,5}, M Hueller^{2,3},
D Nicolodi^{2,3}, S Rowan⁴, D Tombolato^{2,3}, S Vitale^{2,3}, P J Wass^{2,3}
and W J Weber^{2,3}

¹ Centro Fisica degli Stati Aggregati, 38050 Povo, Trento, Italy

² Dipartimento di Fisica, Università di Trento, 38100 Povo, Trento, Italy

³ INFN Gruppo di Trento, 38100 Povo, Trento, Italy

⁴ University of Glasgow, Glasgow G12 8QQ, UK

E-mail: weber@science.unitn.it

Received 31 October 2008, in final form 27 January 2009

Published 20 April 2009

Online at stacks.iop.org/CQG/26/094017

Abstract

On-ground verification of the precision with which a test mass can be in perfect free-fall, without any stray forces, is among the most challenging aspects of preparing for LISA and LISA Pathfinder. This study aims at improving the sensitivity in torsion pendulum measurements of the stray forces arising in the interaction between a test mass and the capacitive position sensor that surrounds it. Measurements are performed with pendulum suspensions based on both tungsten and higher quality factor uncoated fused silica torsion fibers. The results achieved with the fused silica pendulum establish more stringent upper limits on the excess force noise attributable to the sensor—at a level that roughly coincides with the LISA Pathfinder flight goal around 1 mHz. Additionally, these measurements demonstrate a force sensitivity improvement over what can be achieved with thermal noise-limited tungsten over a wide range of frequencies, with significant further improvements still possible.

PACS numbers: 04.80.Nn, 05.40.-a, 07.87.+v, 07.10.Pz

(Some figures in this article are in colour only in the electronic version)

1. Introduction

The LISA gravitational wave mission [1, 2] requires extremely high levels of geodesic purity for the orbits of the nominally free-falling test masses (TMs) that comprise the end mirrors of the three-arm interferometer. The tolerable levels of residual acceleration noise—roughly $3 \text{ fm s}^{-2} \text{ Hz}^{-1/2}$ at frequencies from 0.1 to 3 mHz, or an equivalent force noise of $6 \text{ fN Hz}^{-1/2}$

⁵ Present address: LIGO project, California Institute of Technology, 18-34, Pasadena, CA 91125, USA.

for the envisioned TM of roughly 2 kg—are well below the requirements of the most ambitious free-fall missions currently preparing for launch, including the Microscope equivalence principle test [3] and the GOCE geodesy mission [4], both of which aim at $\text{pm s}^{-2} \text{Hz}^{-1/2}$ acceleration noise in the mHz band. As such, the feasibility of LISA, and its legitimacy as an observatory for gravitational wave astrophysics, must be established with detailed analysis of relevant force noise sources backed up with experimental proof.

A two-pronged approach, in an orbit and on the ground, has been adopted for experimentally probing the limits of free-fall for LISA. The LISA Pathfinder (LPF) mission [5], to be launched in the 2010 time frame, aims at a full flight test of the acceleration noise, at the level of $30 \text{ fm s}^{-2} \text{Hz}^{-1/2}$ at 1 mHz, of a free-falling TM inside a co-orbiting spacecraft under conditions very similar to the final LISA configuration. On the earth, torsion pendulums are used to make high precision measurements of the small force disturbances relevant to LISA free-fall.

Many of the most dangerous and difficult to model force noise sources originate in the interaction between the TM and nearby metallic surfaces of the electrostatic position sensor—or a gravitational reference sensor (GRS)—that surrounds and shields the TM and is used to drive the satellite thruster control loop. Experimental studies have thus focused on this configuration, with a lightweight metallic TM suspended inside a prototype capacitive sensor [6–9] or at least in proximity to representative metallic surfaces [10–12]. Torsion pendulums have served as a crucial ground testbed for preparing, and demonstrating readiness for, the LISA Pathfinder mission, by establishing upper limits on the force noise acting on the LISA TM, characterizing key electrostatic [7, 10] and thermal [9] noise sources for LISA and verifying key in-flight disturbance mitigation techniques, such as photoelectric TM discharge [13] and stray electrostatic field compensation [6].

A recent study [8] placed an upper limit of roughly $100 \text{ fm s}^{-2} \text{Hz}^{-1/2}$ —equivalent to a force noise of $200 \text{ fN Hz}^{-1/2}$ —on the stray acceleration at 1 mHz resulting from unknown surface forces originating in the sensor. This study used representative prototype GRS hardware for LPF, with an Au-coated electrode housing with the LPF flight-model geometry (with 2.9–4 mm gaps between the TM and sensor surfaces) surrounding a LPF-sized 46 mm Au-coated hollow TM and connected to a fully powered LPF sensing and actuation electronics prototype. This upper limit on sensor-related force noise is within a factor of 3 of the LPF acceleration noise goal, and achieving this level in the final LISA mission constellation would be sufficient to allow detection of gravitational radiation from at least several known galactic binary star systems. In these measurements, the total measured force noise acting on the pendulum was, at 1 mHz, roughly twice, in noise power, the Brownian noise arising in the torsion oscillator dissipation, which is dominated by structural losses in the tungsten torsion fiber.

In this paper, we report on improvements in measuring the stray force noise originating in the sensor–TM interaction. The measured data have been obtained for a new prototype sensor featuring Au-coated sapphire electrodes, as in the final LPF design. Measurements have been performed with both a tungsten torsion fiber and the pendulum suspended by an uncoated fused silica fiber. Our measurements show a significant improvement in the force noise obtained with the lower dissipation silica fiber, allowing us to lower the upper limits on possible excess sensor force noise to nearly coincide with the LPF goal.

In addition to the immediate result of improving the force noise limits in preparation for LPF, our study aimed at verifying the feasibility of taking advantage of the lower thermal noise floor of a high- Q fused silica fiber to obtain better torsion pendulum force sensitivity. Recent studies [14, 15] have demonstrated torsional quality factors ranging from roughly 10^4 to 10^6 for fused silica fibers with and without various applied coatings designed to make the

fiber conductive, to avoid possible force noise sources associated with electrostatic charging. These quality factors represent a large potential decrease in the thermal noise floor achieved with tungsten, which is typically of order of several thousands. This study is not a systematic investigation of the pendulum properties as a function of the fiber size or coating. It does however conclusively demonstrate that a clear improvement in force sensitivity is possible with an uncoated fused silica fiber. Additionally, measurements of the pendulum quality factor indicate that a further significant improvement in sensitivity is possible.

2. Experimental apparatus, techniques and measurements

The data presented here are measurements of the pendulum torque noise floor and mechanical quality factor, for two separate integrations of the torsion pendulum. The two integrations differ only in the torsion fiber used, which is made from tungsten in the first and fused silica in the second. Both campaigns employed the same GRS prototype sensor, in the same vacuum chamber and with nominally the same experimental conditions. At the end of the second (fused silica) measurement campaign, a leak in the vacuum chamber was repaired. Given the large decrease in the residual gas pressure—from roughly 3×10^{-4} Pa to 3×10^{-6} Pa—and consequent effect on the measured Q and torque noise, these data are presented separately as ‘high pressure’ and ‘low pressure’ data sets. The experiments presented here represent a portion of a larger test campaign of sensor-related forces in preparation for LPF.

The sensor prototype employed here (shown schematically with the torsion pendulum inertial member in figure 1) is geometrically equal to that used in [8], but the electrode surfaces are realized from sapphire, coated with sputtered Au, rather than the ceramic Shapal. Sapphire was chosen for LPF for its more reliable dielectric properties. The homemade sensor readout and actuation electronics is based on a homemade capacitive-inductive bridge similar in design and performance to that envisioned for LPF.

The torsion pendulum facility is a slightly upgraded version of that described in [8] (the upgrades are detailed in [16, 17]). A double mu-metal magnetic shield, with a low frequency field attenuation factor of roughly 40, has been added inside the vacuum chamber to limit both coupling to the pendulum’s residual magnetic moment (measured to be roughly 10^{-7} Am²) and eddy current damping. Additionally, the mounting of the two readouts of the pendulum torsion angle—the GRS itself and a commercial optical autocollimator—has been improved to limit the readout noise caused by mechanical motion.

The torsion pendulum element—dominated by the 46 mm hollow TM itself (see figure 1) and a mirror used for the autocollimator readout—is unchanged from previous studies. The mass quadrupole moment of the rectangular mirror is nominally compensated by small tuning masses, and by scaling from previous measurements performed in our lab [18], the gravitational noise acting on this pendulum should be negligible.

The electrical isolation of the TM, particularly in light of the use of an insulating fused silica fiber, is worth noting. As in previous studies, and as required for the GRS electrostatic readout, the TM is isolated from the pendulum shaft by a fused quartz ring⁶ designed for extremely high electrical resistance ($\geq 10^{16}$ Ω based on discharge measurements). What does change with the introduction of the fused silica fiber, however, is that the upper stage of the pendulum, including the shaft and mirror, is electrically floating, whereas with tungsten the upper pendulum is grounded through the torsion fiber. While the TM is both well shielded and can be rapidly discharged with a UV light discharge system, the upper pendulum has no electrostatic shield except for the vacuum chamber and is not equipped for UV discharge. The

⁶ Saint-Gobain TSC transparent quartz.

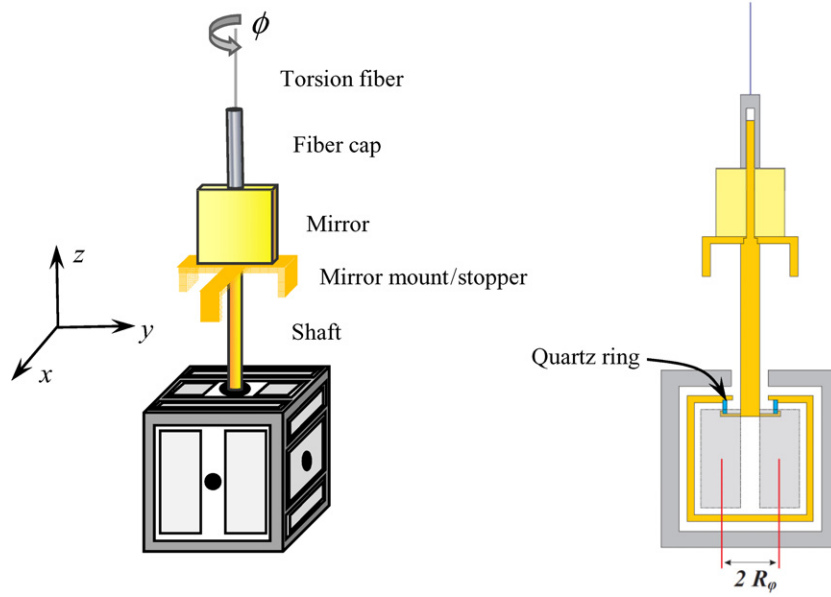


Figure 1. Schematic of the experimental setup, including the torsion pendulum inertial member and GRS prototype. An in-scale yz -plane section at right highlights the TM hanging inside the GRS, with the cubic 46 mm TM connected to the pendulum shaft via an isolating quartz ring. The rest of the inertial member comprises a mechanical stopper, 25 mm gold-coated mirror and a threaded cap, into which the torsion fiber is glued. Also shown in the section at right (in light gray) is the ‘footprint’ of the GRS X face electrodes, used to measure the TM translation x and torsional rotation ϕ , with an effective lever arm $R_\phi = 10.75$ mm. The TM–GRS gaps are 4, 2.9 and 3.5 mm on, respectively, the x , y and z faces. Details of the TM, sensor and overall pendulum apparatus are given in [6–8, 16, 17].

upper pendulum can be discharged—following evacuation of the apparatus, for instance—by rotating the pendulum, via the GRS electrostatic actuation, to make the mirror mount (figure 1) touch mechanical stoppers in contact with the GRS. Additionally, the ambient charging rate of the isolated TM and upper pendulum are slow enough, below 1 elementary charge per second, to not require discharging for months under typical operating conditions.

The fiber used in the first measurement campaign is a nominally $25\ \mu\text{m}$ uncoated tungsten fiber, the same fiber used in [8]. The fused silica fiber was pulled under laser heating at the University of Glasgow. While the fiber apparatus [19] was optimized for pulling thicker, ribbon-shaped fibers for the mirror suspensions of the LIGO gravitational wave observatory, it nonetheless allowed production of a fiber with a roughly circular profile, with a diameter of roughly $40\ \mu\text{m}$, measured to be uniform to within 10% for most of its 1 m length. This was achieved by three repeated pulls with the same material, reducing progressively from a 1.5 mm rod to the final $40\ \mu\text{m}$ fiber. Given the measured yield strengths of the fibers produced—in excess of 3 GPa for typical fibers produced in this range of diameters—this diameter represents a conservative choice for the 110 g torsion element, loading the fiber to less than a quarter of its breaking load (the actual fiber in use was tested for several days with a 300 g load). For both tungsten and silica, the fibers were glued into Au-coated Al caps at each end of the fiber with a conducting epoxy⁷, which were then screwed onto the torsion member and the pendulum upper suspension.

⁷ Epotek H20E silver conducting epoxy.

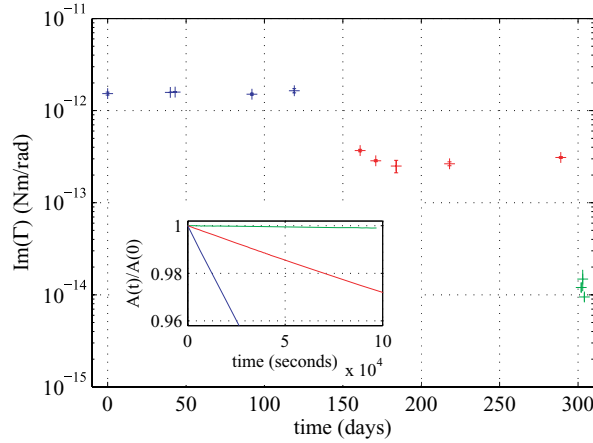


Figure 2. Imaginary part of the elastic constant for tungsten and fused silica pendulums, measured at resonance ($T_0 = 562$ s for tungsten and $T_0 = 465$ s for silica) with the ringdown technique. In order of decreasing imaginary elastic constant, data are shown for tungsten (blue in online version), and for fused silica data (red online) at $(3 \times 10^{-4}$ Pa) and at $(3 \times 10^{-6}$ Pa) (green online). The corresponding average values of Q are 3410 ± 10 for W, and $25\,800 \pm 1300$ and $740\,000 \pm 70\,000$ for fused silica at, respectively, the higher and lower pressure values. The inset shows the beginning of the amplitude decay, normalized to the initial amplitude, for the typical ringdowns with the three data sets.

Typical pendulum torsional constants Γ_0 , calculated from the measured oscillation period T_0 and calculated moment of inertia $I = 4.31 \times 10^{-5}$ kg m², for the tungsten and silica were roughly 5.4 nN m/rad and 7.9 nN m/rad, respectively, with a (negative) contribution of up to several per cent coming from the applied sensor readout voltages.

To calculate the pendulum transfer function and the Brownian thermal torque noise floor, measurements of the pendulum quality factor Q were interspersed with the torque noise measurements. A ringdown technique was used, measuring the decay, for 1–2 days, from a large initial amplitude (typically, several mrad). The quality factor was extracted by fitting the pendulum sine amplitude⁸ to an exponential decay. Uncertainties in the extraction of the resonance quality factor Q —defined $Q = \frac{2\pi}{T_0} \tau$, where τ is the measured energy decay time constant—were determined empirically from the scatter in the measured amplitude derivatives in different cuts of data, typically of length 15 000 s. Weighted averages of the different ringdown results were used for calculating the thermal noise for each data set.

While the ringdown technique measures the quality factor at the resonant frequency, the thermal noise power spectrum depends, for a given frequency, on the effective Q at that frequency:

$$S_{N(\text{th})}(f) = \frac{4k_B T \Gamma_0}{2\pi f Q(f)} \equiv \frac{4k_B T \text{Im}\{\Gamma(f)\}}{2\pi f} \quad (1)$$

with the effective quality factor thus related to the imaginary part of the elastic constant, $[Q(f)]^{-1} = \frac{\text{Im}\{\Gamma(f)\}}{\Gamma_0}$.⁹ The values of the factor $\text{Im}\{\Gamma\}$, relevant to the thermal noise, extracted

⁸ The pendulum angle data were demodulated into sine and cosine components at the resonant frequency, with the phase chosen to make the initial amplitude purely sine. Then the decaying sine amplitude $A_{\sin}(t)$ was fitted to an exponential decay.

⁹ For complex torque and angular amplitudes \tilde{N} and $\tilde{\phi}$, Γ is the generalized elastic constant, $\Gamma \equiv -\frac{d\tilde{N}}{d\tilde{\phi}}$.

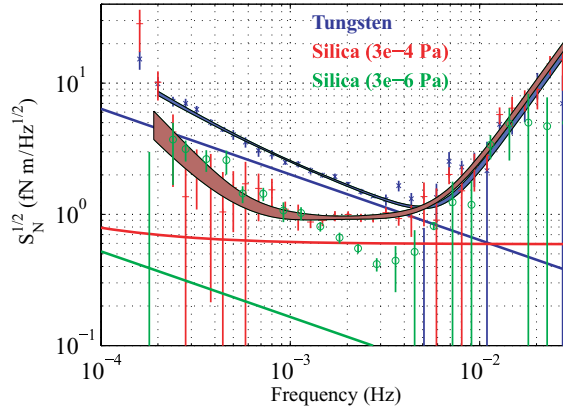


Figure 3. Measured torque noise levels for experimental runs with the tungsten and fused silica fibers, averaged over five and six weekends of data, respectively. Data from a single weekend with the fused silica fiber and low residual gas pressure are also shown, without a fit. In each case, the solid lines represent the calculated thermal noise floor for the respective pendulum.

from the different ringdown measurements are shown in figure 2. In terms of the quality factor Q , we obtain an average of 3410 ± 10 for the tungsten data (for $p \approx 10^{-5}$ Pa), $25\,800 \pm 1300$ for the higher pressure fused silica data and $740\,000 \pm 70\,000$ for the lower pressure fused silica data.

The presence of viscous damping, relevant to the high pressure silica data, produces a Q that decreases with increasing frequency. For the purpose of estimating the frequency-dependent thermal noise background (equation (1)), we parametrize $Q(f)$ in terms of a frequency-independent loss angle δ and a viscous damping decay time τ_v :

$$[Q(f)]^{-1} = \delta + \frac{f T_0^2}{2\pi \tau_v}. \quad (2)$$

A study of Q as a function of frequency, which would allow separate determination of δ and τ , has not yet been possible. However, the huge increase in Q upon decreasing the vacuum pressure for the silica data indicates that the higher pressure silica data are dominated by viscous gas damping. Additionally, given the lower Q measured for tungsten—of order of several thousands as in other studies [8, 20]—even with lower pressure, the tungsten pendulum dissipation comes from the fiber itself, and we thus apply a structural dissipation model, with a frequency-independent loss angle [21]. Finally, given that the viscous gas damping is expected to give $\tau_v \propto Q \propto p^{-1}$, it is likely that gas damping does not, in the frequency range of interest, limit the value of Q at the lower pressures, where a factor of 100 decrease in pressure only gives a factor of 30 improvement in Q . We do not know if the residual dissipation for the low pressure silica data is dominated by structural or viscous damping. For the sake of showing an indicative thermal noise floor for these data in figure 3, we plot a structural damping model anchored to the measurement of Q at the 2.15 mHz resonance frequency, but this choice does not influence any of the conclusions of this paper.

Measurements of the spectrum of torque noise acting on the pendulum, in the presence of the GRS sensor and accompanying electronics, were performed over the course of five and six weekends for, respectively, tungsten and silica (high pressure), with a single weekend of data available for low pressure fused silica. The torque noise acting on the pendulum is obtained by first converting the GRS and autocollimator measurements of the pendulum deflection angle into two torque time series via the pendulum transfer function and then calculating the

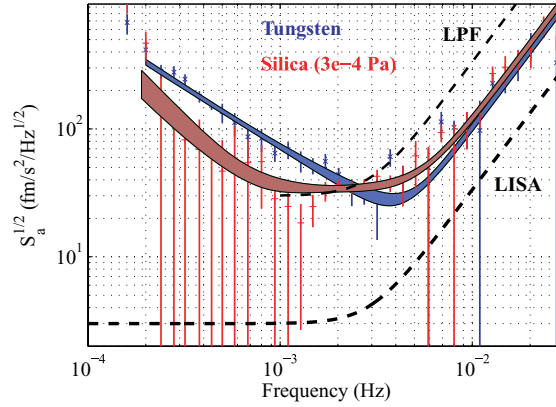


Figure 4. Excess acceleration noise, calculated from the tungsten and fused silica (high pressure) data sets, above the calculated thermal noise background. An effective arm length $R_\phi = 10.75$ mm and a full TM mass of $M = 1.97$ kg have been assumed in converting from torque into acceleration. The dashed black curves correspond to the acceleration noise goals for LISA and LPF.

cross-correlation spectrum [8]. This gives an estimate, $S_N = \text{Re}\{S_{N_{\text{GRS}}, N_{\text{AC}}}\}$, that distinguishes the true torque noise from the uncorrelated measurement noise in the two readouts.

The cross-spectra have been calculated using 25 000 second cuts, overlapped by 50% and each multiplied by a Blackman–Harris window. Data have then been binned logarithmically, in order to have 15 frequency bins per decade. The cuts are then averaged, in noise power, for the two large data sets, with five groups of 16 cuts for the tungsten data and seven groups of 15 cuts for the silica data, with these exact numbers chosen to optimize the use of the 80 and 105 available cuts of data for the two data sets. Finally, averages of these remaining 5 (tungsten) or 7 (silica) data for each frequency bin are then averaged, with uncertainty in each frequency bin based on the scatter in the samples. Performing this two-step averaging process allows an estimate of the uncertainty in the mean of an already averaged spectrum, whose statistical distribution will be more nearly normal than that of a single window spectrum. The same procedure is used for the low pressure fused silica data, where four groups of four data cuts are used, with ten bins per frequency decade.

Averaged torque noise spectra are shown for the different data sets in figure 3, with the background thermal torque noise calculated according to equation (1) and the discussion of the nature of the damping. To guide the eye, we also show fits to appropriate polynomials— f^{-2} , f^{-1} and f^4 for tungsten and f^{-3} , f^{-1} , f^0 and f^4 for the high pressure silica data. No fit or excess acceleration noise estimates are performed for the low pressure silica data, as the limited number of data makes assigning uncertainties unreliable.

The excess noise that could possibly be related to the GRS is computed by subtracting the thermal noise background, as calculated by equation (1), from the measured torque noise. The excess torque noise is converted into force noise by dividing by an arm length $R_\phi = 10.75$ mm, which is half the on-center electrode separation in the sensor and would be the appropriate factor for electronic back-action or other sources which couple through the single GRS electrode (this rather pessimistic choice of converting to force noise is discussed elsewhere [6, 8]). The measurement is not sensitive to force noise sources that do not produce torque noise, such as a force acting only on the center of the TM (a pendulum with direct force sensitivity is discussed in [22]). Finally, this is converted into acceleration noise by dividing by the full TM mass $M = 1.97$ kg (for a 46 mm Au–Pt cube), shown in figure 4 and compared with the related TM acceleration goals for LISA and LPF.

3. Discussion of results

The first conclusion to be drawn from the data, particularly figure 3, is that the uncoated fused silica fiber—even in the lower Q ‘high pressure’ data—allows an improvement in torque sensitivity compared to what can be achieved with a thermal noise-limited tungsten fiber at all frequencies from 0.3 mHz to 6 mHz. The improvement factor for our data is roughly a factor of 6, in power, at 1 mHz. This has been achieved reliably, over a 6 month period, without breaking a fiber or introducing new electrostatic noise sources at levels approaching the tungsten thermal noise floor.

In addition to not introducing extra noise that was not observed with the tungsten pendulum, the measurements with the fused silica fiber actually display *less* excess noise—the measured torque noise in excess of the calculated thermal noise floor—than that observed with the tungsten fiber. This allows a significant improvement, a factor of 3–4 in noise power, in the upper limits of force noise that could be attributed to the GRS. Converted into acceleration noise on the LISA or LPF TM, the upper limit roughly coincides with the LPF goal, in the range of $30\text{--}40\text{ fm s}^{-2}\text{ Hz}^{-1/2}$ at 1 mHz.

The fact that the observed torque noise excess actually decreases upon changing the fiber—with the same GRS and without improving, at least not knowingly, any other environmental noise source—indicates that the tungsten fiber itself contributed excess noise above its calculated thermal noise floor and that we likely underestimate the true background tungsten fiber torque noise. Given the accuracy and reproducibility of the tungsten ringdown measurements—within 1%—it is difficult to associate the noise underestimate—50% in power at 1 mHz—with an error in Q . While a violation of the fluctuation-dissipation theorem is not likely, we note that we do not find data in the literature that confirm the thermal noise prediction for torsion pendulums at mHz frequencies at the level of precision tested here. It is likely that the fiber has some extra, non-equilibrium rotational noise due to the slow relief of some internal stress, which is also suggested by the slow but measurable ‘unwinding’ of the tungsten fiber, typically of order $0.2\text{--}0.3\text{ }\mu\text{rad h}^{-1}$ in our tungsten data.

The large increase in the measured pendulum Q upon repairing the vacuum chamber leak, with an accompanying decrease of a factor of 100 in the measured pressure, implicates gas damping as the dominant pendulum dissipation in the higher pressure data. The quality factor measured at lower pressure is consistent with that measured, at slightly higher frequencies, for other non-coated torsion fibers [15, 14]. We do not know what limits the pendulum Q at these lower pressures, but an investigation of damping from residual gas, electrostatic and magnetic damping sources is planned. Additionally, the flat torque noise floor from 1 to 4 mHz seen in the higher pressure silica data is also consistent with gas damping noise, albeit at roughly twice the noise power calculated with the measured Q of 26 000. Whether or not it is thermal noise, this plateau is indeed associated with the gas leak, as it disappears in the low pressure data set, which gives a torque noise minimum of $0.4\text{ fN m Hz}^{-1/2}$ at 3 mHz.

While the torque noise data measured with the $Q \approx 740\,000$ pendulum represents an improvement over previous pendulums and an important step in characterizing the GRS force noise, they are also well above the calculated thermal noise floor. The source of this noise excess is not known as yet and its investigation is critical, as the possibility that the observed force excess arises in the GRS itself, at a level above the LISA goal, cannot be excluded *a priori*. Analysis of the measured fluctuations in the apparatus inclination, temperature and magnetic field indicate that these sources do not contribute significantly to the measured torque noise.

In addition to a number of possible true torque noise sources, current measurements are limited by the noise in the readout—or readouts—used to measure the pendulum angular

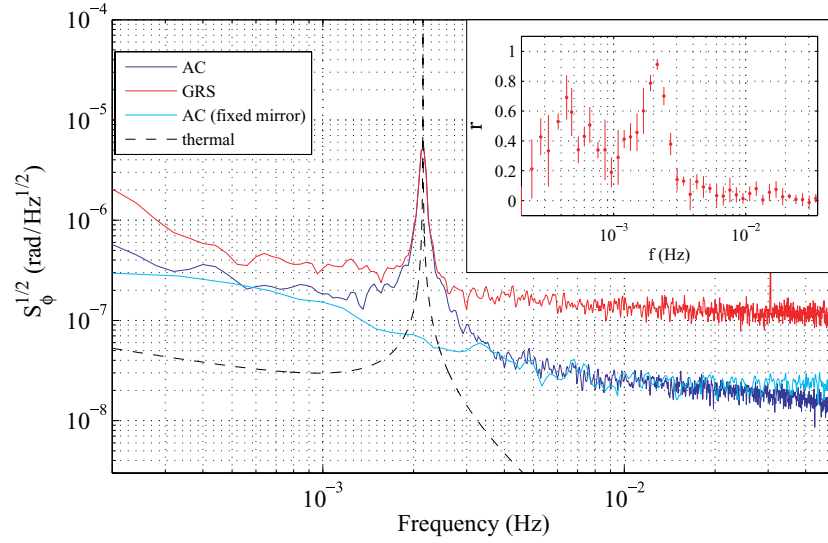


Figure 5. Illustration of a measured autocollimator and GRS angular noise with a fused silica fiber (with $Q \approx 740\,000$). The best measured autocollimator performance in the experimental setup, achieved with a fixed mirror in the place of the suspended pendulum, and the estimated pendulum thermal noise floor are shown for comparison. The electronic noise floor of the GRS is roughly $130 \text{ nrad Hz}^{-1/2}$. The measured broadening of the resonant peak is an artifact of the short (25 000 s) spectrum window. The inset shows, for the same data set, the cross-coherence—defined $r \equiv \text{Re}\{S_{N_{\text{GRS}}, N_{\text{AC}}}\}/[S_{N_{\text{GRS}}} \times S_{N_{\text{AC}}}]^{1/2}$ —which shows that the two readouts approach a near perfect correlation only close to the pendulum resonance where displacement is largest. While the cross-correlation analysis technique, used for figures 3 and 4, discriminates the readout noise from true pendulum motion, the readout noise introduces significant uncertainty in our excess force noise estimate.

deflection. Figure 5 shows how neither the autocollimator nor GRS is able, alone, to resolve the fused silica thermal noise floor. While the torque noise excess can be identified, with the averaged cross-spectrum data analysis technique employed here, at levels below the noise floor of the single readouts, readout noise adds uncertainty to the estimates and complicates any debugging of true force noise sources. Some improvement is possible with a smaller diameter fused silica fiber, which reduces the impact of the readout by allowing larger displacements for a given torque. However, for the long-term development of the pendulum, we intend to implement an interferometric angular readout. Differential wavefront sensing, to be used for LISA and LPF [23], has already demonstrated sensitivity below $10 \text{ nrad Hz}^{-1/2}$ at mHz frequencies and represents a potential starting point design for a high precision torsion pendulum angular readout.

References

- [1] Bender P *et al* 2000 LISA: a cornerstone mission for the observation of gravitational waves *ESA-SCI(2000)11 System and Technology Study Report*
- [2] Vitale S *et al* 2002 *Nucl. Phys. B* **110** 209–16
- [3] Hudson D, Chhun R and Touboul P 2007 *Adv. Space Res.* **39** 307–14
- [4] Drinkwater M D *et al* 2007 *Proc. 3rd Int. GOCE User Workshop (ESA SP-627)* pp 1–8
- [5] Anza S *et al* 2005 *Class. Quantum Grav.* **22** S125–138
- [6] Carbone L *et al* 2003 *Phys. Rev. Lett.* **91** 151101

- [7] Carbone L *et al* 2005 *Class. Quantum Grav.* **22** S509–519
- [8] Carbone L *et al* 2007 *Phys. Rev. D* **75** 042001
- [9] Carbone L *et al* 2007 *Phys. Rev. D* **76** 102003
- [10] Pollack S E, Schlamminger S and Gundlach J H 2008 *Phys. Rev. Lett.* **101** 071101
- [11] Schlamminger S *et al* 2006 *Proc. 6th Int. LISA Symp. (AIP Conf. Proc. vol 873)* (New York: AIP) pp 151–7
- [12] Pollack S E, Schlamminger S and Gundlach J H 2006 *Proc. 6th Int. LISA Symp. (AIP Conf. Proc. vol 873)* (New York: AIP) pp 158–64
- [13] Wass P J *et al* 2006 *Proc. 6th Int. LISA Symp. (AIP Conf. Proc. vol 873)* (New York: AIP) pp 220–4
- [14] Hagedorn C A, Schlamminger S and Gundlach J H 2006 *Proc. 6th Int. LISA Symp. (AIP Conf. Proc. vol 873)* (New York: AIP) pp 189–93
- [15] Numata K, Horowitz J and Camp J 2008 *Phys. Lett. A* **370** 91–8
- [16] Tombolato D 2008 Laboratory study of force disturbances for the LISA Pathfinder free fall demonstration mission *PhD Thesis* Università di Trento
- [17] Nicolodi D 2007 Toward a third generation torsion pendulum for the femto-Newton level testing of free fall in the laboratory *Masters Thesis* Università di Trento
- [18] Carbone L *et al* 2006 *Proc. 6th Int. LISA Symp. (AIP Conf. Proc. vol 873)* (New York: AIP) pp 561–5
- [19] Heptonstall A *et al* 2007 *Proc. 42nd Recontres de Moriond, Gravitational Waves and Experimental Gravity* ed J Dumarchez and J T T Van (Hanoi, Vietnam: The Gioi Publishers)
- [20] Kapner D J *et al* 2007 *Phys. Rev. Lett.* **98** 021101
- [21] Gonzales G I and Saulson P R 1995 *Phys. Lett. A* **201** 12–8
- [22] Cavalleri A *et al* 2009 *Class. Quantum Grav.* **26** 094012
- [23] Wand V *et al* 2006 *Class. Quantum Grav.* **26** S159–167